

# Immunity of Automotive Power Line Communication Systems

Alexander Zeichner and Stephan Frei, *Senior Member, IEEE*

**Abstract**—Power line communication (PLC) could not be established in automotive environments till now due to concerns with the unavoidable electromagnetic disturbances in the vehicle supply nets. Conducted broad band switching noise and field coupled narrow band noise can disturb the communication and prevent higher data rates. The continuously increasing size of the communication cable harnesses in vehicles is very difficult to handle, and PLC could reduce the complexity of the harness. This paper presents an approach to estimate the theoretical limits of PLC in the presence of noise in automobiles. Signal power and bit error rates are computed and discussed, based on electromagnetic compatibility-standards and PLC-parameter sets from older investigations' noise levels. Commonly used automotive immunity tests are applied to analyze the signal to noise ratio of the PLC in a simulation environment. Therefore, immunity test setup models are introduced in order to analyze the noise injection and coupling characteristics to the PLC receiver. A virtual direct power injection (DPI) test is carried out with narrow band noise and transient pulse injection. For method validation, BCI measurements of a real PLC transceiver were carried out and failure behavior was compared to DPI simulation results. Immunity improvement for single carrier modulation in PLC is proposed. Finally, an analysis of the immunity to pulses is performed and results are discussed.

**Index Terms**—Electromagnetic compatibility (EMC), immunity test, in-vehicle power line communication, power line communication (PLC).

## I. INTRODUCTION

THE demand for more functions in automobiles leads to a higher number of electronic control units (ECUs), actuators, and sensors. These systems are distributed over the entire vehicle and need an interconnection for data exchange. Traditionally used bus systems are local interconnect network (LIN), controller area network, FlexRay, and vehicle-Ethernet for very high data rate applications. These data transmission systems need one or more dedicated communication cables for data transfer. Besides these cables, every ECU needs to be connected to the 12 V power supply network. The wiring harness complexity, weight, and volume growth as a result of the increasing number of systems. To reduce the complexity and weight, simultaneous use of supply cables for power and data transmission is an interesting solution. The power line communication (PLC)

Manuscript received March 15, 2016; revised May 23, 2016; accepted June 05, 2016. Date of publication June 28, 2016; date of current version July 22, 2016. This paper is for the Special Issue and is an expanded version from the 2015 IEEE Symposia from Santa Clara or Dresden.

A. Zeichner is with the On-board Systems Lab, Technische Universität Dortmund Fakultät für Elektrotechnik und Informationstechnik, Dortmund 44227, Germany (e-mail: alexander.zeichner@tu-dortmund.de).

S. Frei is with the On-board Systems Lab, TU Dortmund University, Dortmund 44227, Germany (e-mail: stephan.frei@tu-dortmund.de).

Color versions of one or more of the figures in this paper are available online at <http://ieeexplore.ieee.org>.

Digital Object Identifier 10.1109/TEMC.2016.2579665

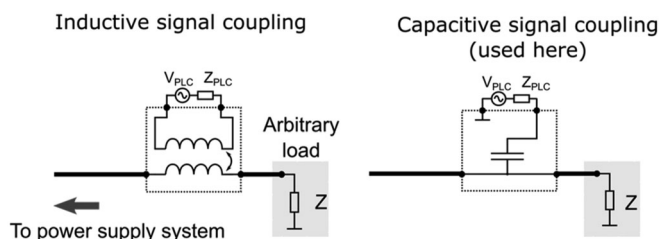


Fig. 1. Inductive and capacitive coupling of PLC signal sources in a power supply system. The same coupling circuits can be used for the receiver.

can often be found in industrial applications or private homes for internet access over the ac low-voltage grid. A new application for PLC could be vehicles [1] or aircrafts [2]. PLC faces different challenges when implemented in a vehicle energy supply network.

Coupling circuits are required for coupling the PLC signal to the power supply system and blocking the 12-V dc voltage from the transceiver input. Investigations on the circuits for differential mode signaling are performed in [3] and [4], and these can be applied to differential dc busses. Signal coupling and decoupling to the automotive power supply system requires circuits for single wires. The coupling circuit variations are depicted in Fig. 1 including capacitive and inductive coupling circuits. A combination of both circuits is also possible. The figure shows a PLC signal source that consists of a voltage source  $V_{PLC}$  and internal source impedance  $Z_{PLC}$  connected to an arbitrary load  $Z$  in the 12-V power supply system. The total impedance of  $Z_{PLC}$ , the coupling circuit and load  $Z$  should be close to the characteristic impedance of the transmission line, to achieve good signal transmission characteristics.

Several publications discuss the integration of PLC in typical vehicular dc power supply systems [1], [5], [6]. Coexistence of PLC and other systems in the power distribution network require a good understanding of the channel transfer function and the unavoidable high noise levels. The integration of PLC in vehicles needs to manage variations of channel transfer properties and must consider that many frequencies are used already for vehicle-internal functions [7], [8].

The power line channel is noisy due to the switching actions that are often controlled with power electronics. Pulses must be assumed to occur randomly in the power supply system and were modeled mainly with statistical methods [9], [10]. The channel properties are as important as the modulation schemes that are used in PLC [11], [12].

Detailed vehicle PLC radiation analysis cannot be found in the literature for frequencies below 30 MHz. One reason might be the missing legal demands here. Electromagnetic

compatibility (EMC) thresholds below 30 MHz are not defined, e.g., in the European Regulation document ECE R-10 [13]. As the frequency band from 1.8 MHz up to 30 MHz is often unallocated in automobiles, PLC could be used in this frequency range without conflicting with internal services or legal demands. For evaluation of the required immunity of an automotive PLC application, an analysis of the internally conducted noise that has to be expected is needed. Therefore, a theoretical analysis of the conducted noise levels in the power supply system based on conducted emission limits for ECUs from CISPR 25 [14] is carried out in Section II, and the required signal power and bit error rate (BER) are proposed. Standard automotive immunity tests [15], [16] are used for assessing the immunity behavior of PLC systems for operation in a vehicular power supply system. Usually continuous wave (CW) signals or transient pulses are injected into the channel between transmitter and receiver. In Section III, typical automotive immunity tests are modeled and their transmission characteristics, between the noise injection port and the PLC receiver terminals, are analyzed and discussed with respect to the previously estimated noise power in the electrical system. Additionally, PLC input filters are examined in combination with the test setups and discussed. In Section IV, a virtual DPI immunity test with amplitude shift keying (ASK)-based transmitter and receiver models is performed and compared to BCI measurement results. Proposals for immunity level optimization of the PLC system are investigated. Additional transient pulse tests are carried out and simulation results are analyzed. The paper closes with a conclusion.

## II. THEORETICAL ANALYSIS

In the performance analysis of communication systems, the signal to noise ratio (SNR) is a significant value to estimate the required bandwidth and data rate. According to [17] the relation is given by

$$C = W \cdot \log_2 \left( 1 + \frac{P}{N} \right). \quad (1)$$

The equation describes the theoretical data rate  $C$  in the presence of white noise where  $W$  is the available channel bandwidth,  $P$  is the signal power, and  $N$  is the noise power. Based on this fundamental equation from communication theory, the physical limitations of a communication system can be estimated for certain requirements. Theoretical approximations of noise in automotive power supply systems and a presentation of BER's dependence on SNR are carried out in the following sections. From requirements of BER and transmission power, the bandwidth or data rate can be calculated with (1) and allow a suitable filter design, choice of modulation scheme, and frequency band.

### A. Theoretical Approximation of Noise in Power Supply Systems Based on Automotive EMC Test Standards

As described in the introduction, the noise characteristics of an automotive 12-V power supply system were analyzed in many publications. On power lines, a certain level of conducted noise is to be expected, mainly due to the use of switched mode converters, mode switching, and on/off transients for the lower

frequencies. At higher frequencies, the digital systems of the ECUs are mainly responsible for the noise. It is challenging to find a general description for noise in such an automotive system. To find the general operation limitations for PLC in automotive environments, it is necessary to have estimations of the noise level. This level is usually controlled and limited by EMC standards in cases of conducted emissions. Limits from such EMC test standards can be helpful in finding an approximation. In this investigation, the noise limits can be seen as a worst-case scenario that must be assumed in the supply system. PLC should operate with a suitable SNR, which will be discussed in Section II-B. Component test standards, e.g., CISPR 25 [14], are applied to protect receivers from disturbances produced by conducted and radiated emissions in a vehicle. Limits for conducted emissions from the electrical systems of a vehicle are given in such a standard. It is assumed here that these limits can be used to calculate the maximum noise level that can occur in a power supply system. In this calculation, it is also assumed that the given maximum voltage level is measured by an ideal test receiver with an internal resistance of  $50 \Omega$ . At higher frequencies, an ideal artificial network of CISPR 25 should behave like that. The noise power spectrum density (PSD) can then be calculated by

$$N_0(f) = \frac{V(f)^2}{50 \Omega}. \quad (2)$$

The frequency dependent voltage  $V(f)$  is the absolute root mean square (RMS) value and  $N_0(f)$  is the distributed noise power among the various frequencies. Suppose that the PLC transmitter and receiver operating in a frequency band  $W = f_2 - f_1$ , then the total received noise power can be calculated by the integration of the noise PSD

$$N = \int_{f_1}^{f_2} N_0(f) df. \quad (3)$$

In cases where the PSD is constant, the noise power can be calculated by a simple multiplication of the PSD from the considered frequency band and applied bandwidth  $W$ .

In CISPR 25, the defined voltage levels are constant for each frequency band. Interpolation and calculation with (2) results in a continuous noise PSD. Fig. 2 shows the calculated noise PSD from four relevant frequency bands based on the class 1 average limits given in [14].

The maximum conducted noise level can be expected to be between  $-17$  dBm/Hz for 150 kHz down to  $-60$  dBm/Hz for 50 MHz. To point out the absolute values determined in Fig. 2, the produced power of a signal source with  $50 \Omega$  of internal impedance and matched termination can be compared. An internal RMS voltage of  $0.5$  V would produce a power of  $7$  dBm. Proposals of the required SNR are given in the next section.

### B. Theoretical BER Analysis and Signal Power Estimation

The SNR can be applied to calculate the BER for a given modulation scheme. From digital communication theory, e.g., [18], the BER for ASK, frequency shift keying (FSK), and phase

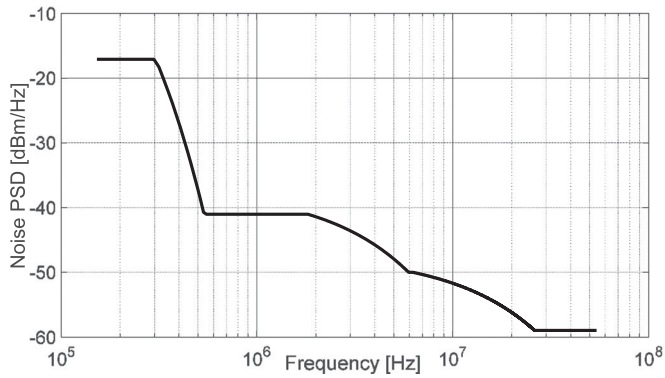


Fig. 2. Maximum noise PSD to be expected in an automotive power supply system is based on the limits of the averaged class 1 voltage levels for conducted emissions from [14].

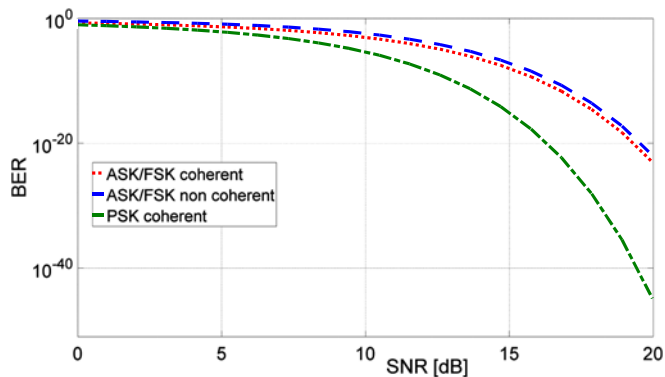


Fig. 3. Theoretical BER over SNR for coherent ASK/FSK/PSK and noncoherent ASK/FSK modulation schemes.

shift keying (PSK) can be expressed by

$$\text{BER}_{\text{Coh. ASK/FSK}} = \frac{1}{2} \text{erfc} \left( \sqrt{\frac{E_b}{2N_0}} \right) \quad (4)$$

$$\text{BER}_{\text{N.Coh. ASK/FSK}} = \frac{1}{2} e^{-\frac{E_b}{2N_0}} \quad (5)$$

$$\text{BER}_{\text{Coh. PSK}} = \frac{1}{2} \text{erfc} \left( \sqrt{\frac{E_b}{N_0}} \right). \quad (6)$$

The probability of error is described by the complementary error function  $\text{erfc}$ . The ratio  $E_b/N_0$  is the SNR, where  $E_b$  is the bit energy, and  $N_0$  is the noise PSD. The BER formulas for coherent ASK/FSK (4) and coherent PSK (6) differ in terms of SNR. To reach the same BER, an SNR that is 3 dB higher than the previous SNR is required for coherent ASK/FSK modulation. The BERs for the considered modulation schemes are compared in Fig. 3.

Some restrictions can be defined as a result of theoretical analysis. For operation estimations of PLC in an automotive power supply system, an SNR of 20 dB is assumed. This means that the standard limits will be exceeded by 20 dB. As a result, the PLC will not be compliant to the standard. A proper assumption is that for a small selected PLC frequency band, the limits can

be raised because there are several frequency bands that are normally not used for automotive communication. Meanwhile, the higher limits would not affect in-vehicle functions. Harmonics from a nonideal PLC signal source outside of the transmission band can be suppressed by an appropriate filter. Radiated far field limits are much higher anyway, and they do often not correlate well with conducted vehicle limits. Consequently, the PLC system can achieve a probability of error of less than  $10^{-20}$  for an ASK/FSK/PSK modulation scheme (see Fig. 3), which leads to a very reliable communication link. A frequency band close to a carrier frequency of 6.5 MHz can be chosen according to an available PLC transmitter for automotive applications. In that band, a noise PSD of  $-50$  dBm/Hz (see Fig. 2) can be assumed to obtain the necessary signal power of approximately  $-30$  dBm for achieving the SNR of 20 dB. The band choice furthermore depends on the channel noise and the transfer characteristics in terms of signal attenuation. Finally, the lower signal power boundary is limited by the noise and target BER. The upper boundary is restricted by the power consumption and radiation limits for external broadcasting services. Here, it is assumed that 20 dB above the vehicle's internal conducted limits will not cause conflicts in some selected frequency bands.

### III. AUTOMOTIVE IMMUNITY TESTS SETUP ANALYSIS

Conducted or radiated EMC immunity tests for components provide an upper limit of disturbances to be expected in automotive environments that can affect the PLC. Three commonly used test setups for capacitive (DPI), inductive (BCI), and field coupling were investigated. For the PLC system, it can be assumed that the test setup is the noisy channel, and the coupling between the injected and received noise power at the transceiver terminal can be analyzed. Furthermore, the system consists of an input filter in the receiver. The components in the frequency domain are described by frequency dependent transfer functions. The channel transfer function describes the transfer characteristics from the noise injection port to the receiver port. The received signal  $R(f)$  is determined by multiplying the injected noise  $N(f)$  by the channel transfer function  $G_c(f)$  and the receiver input filter transfer function  $G_{\text{Rx}}(f)$

$$R(f) = G_{\text{Rx}}(f) \cdot G_c(f) \cdot N(f). \quad (7)$$

The following analysis primarily considers the transfer characteristics ( $G_c(f)$ ) of the test setups. Estimations of the coupled noise power at the receiver impedance can be performed. Results will be discussed according to the necessary signal power for an appropriate BER under conducted and radiated EMC component immunity test conditions. The developed models will be applied in further virtual immunity tests. The complete system investigations will be carried out in Section IV.

#### A. BCI and DPI Forward Power Coupling Model

The analyzed automotive immunity test setups for components can be replaced by a three-port passive network, which can be described by scattering parameters. Two ports are terminated by the transmitter and receiver impedances. One port is

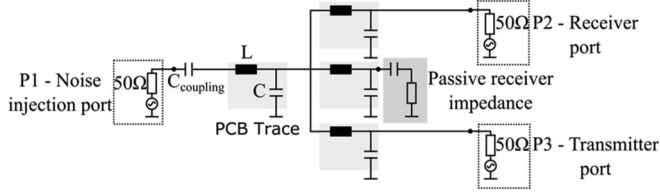


Fig. 4. Three-port DPI circuit model consisting of a coupling capacitance  $C_{\text{coupling}}$  (47 nF) for noise injection and L- and C-elements (50 nH/5 pF) to model the traces of 5 cm length on the PCB. According to [16] three transceivers have to be considered. A transmitter and receiver can be attached at P2 and P3. The third transceiver is considered as a passive receiver impedance consisting of a resistor (1 MΩ) in series with a coupling capacitor (1 nF).

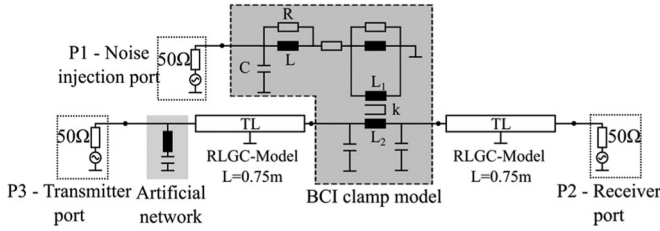


Fig. 5. Three-port BCI circuit model. The BCI clamp is modeled by a mutual inductance ( $L_1 = 4.3 \mu\text{H}$ ,  $L_2 = 5.12 \mu\text{H}$ ,  $k = 0.9933$ ), and parasitic effects were considered by R-, L- C-elements. RLGC transmission line models with 0.75 m length are attached to the BCI clamp model terminals. An artificial network according to [14] is attached at the transmitter port.

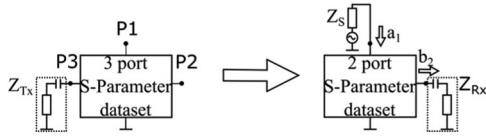


Fig. 6. Three-port dataset recalculation to a two-port dataset, considering the transmitter and receiver impedances.

applied to inject the disturbance power. The circuit models for the BCI and DPI test setups are introduced in Figs. 4 and 5.

The upper band limit that is typically used in broadband PLC is 30 MHz. The greatest influence of noise can be expected in this band. Other effects in higher frequencies, caused by the internal physical transceiver structure, are neglected. Consequently, S-parameter circuit simulation was performed in the extended frequency range of 300 kHz to 50 MHz, and the simulation dataset was extracted for further postprocessing. Transmitter impedance  $Z_{\text{Tx}}$  is virtually attached to port P3 of the original dataset to obtain a two-port dataset (see Fig. 6).

$Z_{\text{Tx}}$  and  $Z_{\text{Rx}}$  both include coupling capacitors of 1 nF in series with the internal impedances. The internal transmitter source impedance was set to 50 Ω, and the receiver input impedance is 1 MΩ to reproduce the high input impedance of an amplifier. The transfer function can be calculated by [19]

$$H_C = \frac{b_2}{a_1} = \frac{\sqrt{\text{Re}(Z_{\text{Rx}}) \text{Re}(Z_s)}}{Z_{\text{Rx}}} \frac{S_{21} (1 + \Gamma_{\text{Rx}}) (1 - \Gamma_s)}{(1 - S_{22} \Gamma_{\text{Rx}}) (1 - \Gamma_{\text{in}} \Gamma_s)} \quad (8)$$

where  $\Gamma_{\text{Rx}}$  and  $\Gamma_s$  are the reflection coefficients of the attached receiver impedance  $Z_{\text{Rx}}$  and the source impedance  $Z_s$ .  $\Gamma_{\text{Rx}}$ ,

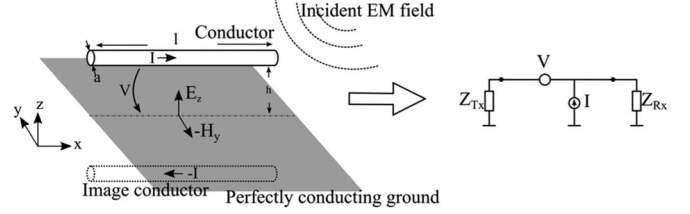


Fig. 7. Geometry of a conductor over ground, excited by an incident electromagnetic field (left) [20]. Excitation is modeled as lumped current and voltage sources are connected to the transceiver impedances (right).

$\Gamma_s$  and  $\Gamma_{\text{in}}$  can be calculated by

$$\Gamma_{\text{Rx}} = \frac{Z_{\text{Rx}} - Z_0}{Z_{\text{Rx}} + Z_0}, \quad \Gamma_s = \frac{Z_s - Z_0}{Z_s + Z_0}$$

$$\Gamma_{\text{in}} = S_{11} + \left( S_{12} S_{21} \frac{\Gamma_{\text{Rx}}}{1 - S_{22} \Gamma_{\text{Rx}}} \right). \quad (9)$$

### B. Field Coupling Model

Radiation immunity tests for automotive components can be performed in absorber lined shielded enclosure (ALSE) on a metallic table. For frequencies up to 30 MHz, the wire is electrically short, ( $l < \lambda$ ) and any propagation effects can be neglected. Hence, a simple low-frequency model is applied to calculate the coupled power at the receiver impedance. A single wire (radius 2 mm) of 1 m length and 5 cm height above a perfectly conducting ground is assumed (see Fig. 7, left). Here, the simulations were performed up to 50 MHz. Although the accuracy cannot be expected to be high any more, the basic behavior still can be represented. The height ( $h$ ) and length ( $l$ ) have an impact on the current and voltage of the wire and were chosen according to the typical antenna tests that were performed in anechoic chambers.

The induced voltage and influenced current on the wire can be modeled as lumped voltage and current sources (see Fig. 7, right). Consequently, the relation to the incident field values can be expressed by following equations from [20, p. 345]:

$$V = -j\omega\mu_0 l h H_y \quad (10)$$

$$I = -\frac{j\omega\pi\epsilon_0 l 2h}{\ln\left(\frac{2h}{a}\right)} E_z. \quad (11)$$

The incident electromagnetic field components are denoted as  $E_z$  and  $H_y$ . The following equation for transfer function can be found by attaching transceiver impedances  $Z_{\text{Tx}}$  and  $Z_{\text{Rx}}$  to the equivalent sources

$$H_{C,\text{Field}} = \frac{P_{\text{Rx}}}{E} = \left( -\frac{j\omega\mu_0 l h}{377\Omega} - \frac{j\omega\pi\epsilon_0 l 2h}{\ln\left(\frac{2h}{a}\right)} \cdot \frac{Z_{\text{Tx}} Z_{\text{Rx}}}{Z_{\text{Tx}} + Z_{\text{Rx}}} \right)^2 \quad (12)$$

The field coupling transfer function describes the received power  $P_{\text{Rx}}$  at the attached  $Z_{\text{Rx}}$ , excited by the electromagnetic field. Far field conditions are assumed. Furthermore, the proposed model uses the orientation of the incident plane wave ( $E$ -field is oriented in  $z$ -direction and  $H$ -field in negative  $y$ -direction) to achieve maximum coupling. This, and the far field

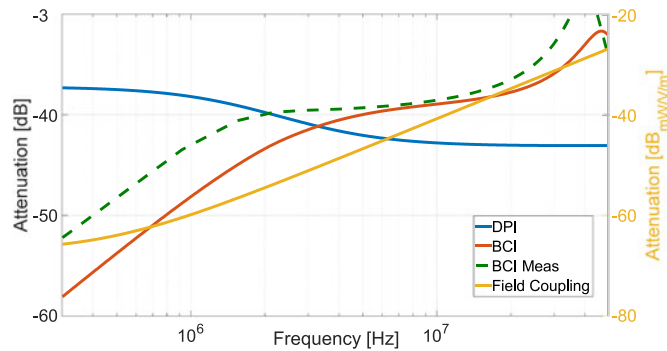


Fig. 8. Comparison of the coupling transfer functions between the injection port of the coupling system and the receiver input impedance.

assumption, does not comply with a test in ALSE but might reflect better reality.

### C. Attenuation Functions and Comparison to Noise Level in Power Supply Systems

The attenuation of the coupling transfer functions which were introduced before, are shown in Fig. 8. Additionally, a three-port S-parameter measurement of a BCI setup is shown for validation.

The BCI model (red solid line) shows a constant deviation to the measurement (green dotted line) of approximately 7 dB below 2 MHz. A close match to the measurements from 2 to 20 MHz can be observed. The resonance from the BCI setup at 40 MHz is reproduced by the model with less than 7 dB deviation. The model was not improved further since different BCI-clamps show different behavior, and the purpose of these investigations are general statements on PLC.

Maximum noise level in the supply system (see Fig. 2) at the frequency of 6.5 MHz can be expected around  $-50$  dBm/Hz. At that frequency, the coupling transfer functions for BCI and DPI simulations have the attenuation of  $-40$  and  $-45$  dB, respectively. To reach the noise level of  $-50$  dBm/Hz in the BCI/DPI simulation, an injected forward power of  $-10$  dBm to the BCI injection port and  $-15$  dBm to DPI port (respectively) are required. Typically, the tests are performed with a much higher injection of forward power which results in a much higher noise at the receiver. Automotive ALSE tests are performed with field strength up to 200 V/m (46 dBV/m) and would lead to a noise level of approximately 2 dBm at the receiver. It can be concluded that the immunity of the PLC transceivers in such component tests need to meet much higher requirements than those for operation in the noisy power supply system. As disturbances are expected to be narrow-banded, further operational strategies can be derived to meet the requirements from the EMC immunity test standards.

### D. Receiver Input Filter

Input filters are important EMC countermeasures and often used in communication systems to separate the signal from broad band noise. Two filters are examined here. A simple

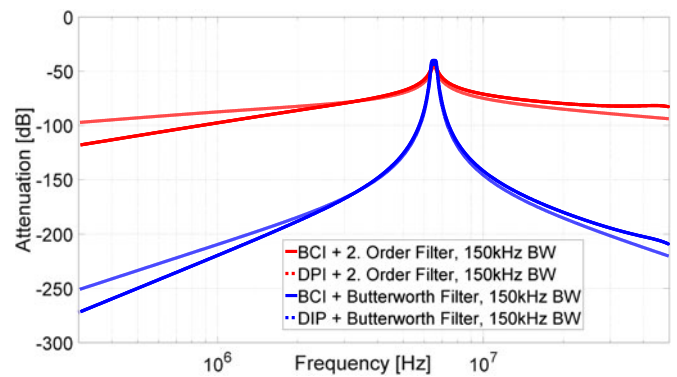


Fig. 9. Transfer function of the BCI/DPI test setup in combination with different receiver input filters (second-order BP filter and Butterworth filter).

second-order input filter, which can be described in the frequency domain by this transfer function

$$G_{Rx}(s) = \frac{b_1 s}{a_2 s^2 + a_1 s + 1}. \quad (13)$$

Furthermore, a more complex Butterworth filter is comparatively investigated, which is described by a rational eighth-order transfer function

$$G_{Rx}(s) = \frac{b_4 s^4}{a_8 s^8 + a_7 s^7 + \dots + a_2 s^2 + a_1 s + 1}. \quad (14)$$

This filter has a considerably steeper profile and a flat pass-band. Similar properties have commercially available ceramic filter. The coefficients  $a_i$  and  $b_i$  determine the center frequency and the filter bandwidth.

According to (7), the calculation results of the noise transmission from the immunity test setups, combined with the input filters, are depicted in Fig. 9. Main objective of the complete setup analysis is to investigate and compare the noise transfer behavior of two different filters in combination with the used immunity test setups (BCI and DPI). Here, the 6.5 MHz band was chosen as the center frequency of the bandpass (BP) filters. Additionally, the filters have a 3-dB bandwidth of 150 kHz.

The results show a significant coupling of noise through the passband of the PLC input filters. The characteristic filter attenuation outside of the passband dominates and the BCI and DPI setups have only minor impact. By injecting a noise signal of 10 dBm in the passband of the receiver input filter, when a signal power of  $-30$  dBm is assumed, the SNR can be reduced to zero. This can lead to considerable disturbances in the communication. Injecting noise outside of the passband would require more power to achieve a magnitude that may impede the demodulation. In the next chapter, a virtual DPI immunity test of the complete low data rate PLC system is shown.

## IV. TRANSCEIVER IMMUNITY TEST

Investigations in this section focus on low data rate signal transmission, comparable to LIN-bus. Theoretical performance limits of PLC will be compared to measurement results. Therefore, ASK transmitter and receiver models are introduced. A virtual DPI test that is typically used for testing LIN transceivers

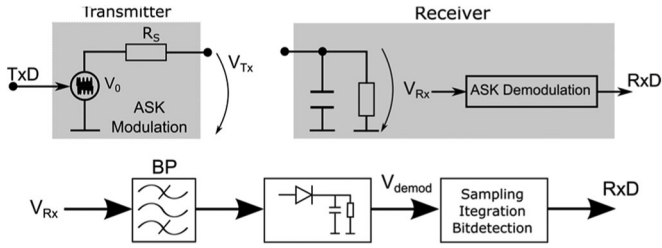


Fig. 10. Implemented ASK model with noncoherent demodulation.

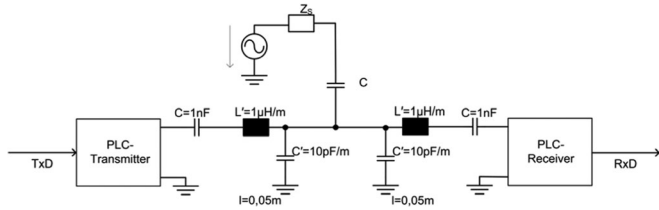


Fig. 11. Complete DPI simulation setup.

[16] is performed with the models. Additionally, a real BCI test is performed for a Yamar transceiver which applies PSK modulation. In the tests, CW disturbance signals were injected. Furthermore, a virtual pulse test is performed.

A. Transmitter/Receiver Model and Virtual DPI Test Setup

Both impedances of the transmitter and the receiver are modeled as shown in Fig. 10 with a linear equivalent circuit where TxD denotes the digital data signal,  $V_{Tx}$  represents the voltage at the transmitter output,  $V_{Rx}$  is the voltage at the receiver input, and RxD is the received digital data signal.

The transmitter is assumed to be an ideal voltage source with an internal source resistance  $R_s$  of  $50 \Omega$ . The source mathematically generates a modulated carrier signal which is dependent upon on the binary TxD signal connected to the source. A frequency of 6.5 MHz for the carrier signal were chosen according to the theoretical analysis in II.

The input impedance is assumed as a combination of a resistor and a capacitor in parallel. The resistor represents the high impedance input ( $1 \text{ M}\Omega$  here) of an amplifier inside of the transceiver chip with a parasitic capacitance of 10 pF. Nonlinearities are neglected in these models.

The received voltage  $V_{Rx}$  will be postprocessed by a demodulation method to detect the binary data in  $V_{demod}$ . Noncoherent ASK demodulation is used in the model to keep the structure as simple as possible. The receiver model is composed of BP filters and an envelope detector. The simple envelope detector used here is a circuit, containing a diode and a low pass filter to suppress the carrier signal. In order to detect the digital bit stream, the demodulated signal  $V_{demod}$  is sampled and compared with a decision threshold at half of the received voltage, three times per bit. A majority decision is performed for the sampled value to detect the bit value.

The complete, detailed virtual DPI simulation setup is depicted in Fig. 11. The ASK transmitter and receiver are attached to the DPI coupling circuit, which is similar to the previously analyzed coupling circuit in Section III, Fig. 4. In the test procedure, a sweep of frequency and forward power is performed.

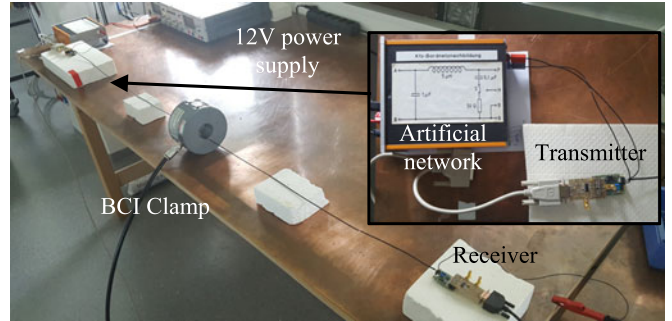


Fig. 12. BCI measurement setup.

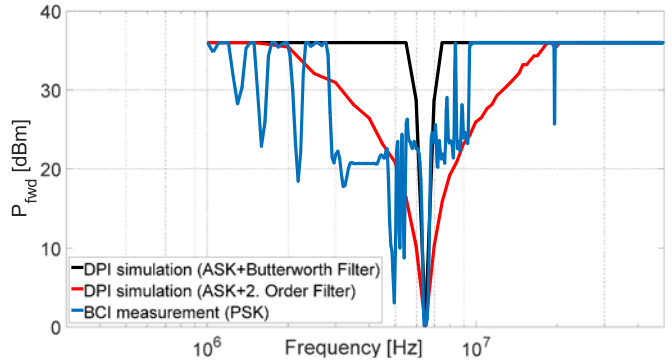


Fig. 13. Comparison of the implemented ASK model disturbance limits for the DPI test with different input filters.

A bit pattern is transmitted at every step of frequency and forward power. In case of a transmitted and received data mismatch, the maximum immunity level at the achieved frequency and forward power is exceeded. In the presented simulations, the virtual test is performed in the frequency range of 1 to 50 MHz.

B. Simulation and Measurement Results

The results of the performed DPI test, in combination with the transmitter and receiver models, can be seen in Fig. 13. These tests were carried out according to the LIN EMC test specification [16]. CW disturbance signals, with a maximum forward power of 36 dBm, were used. Additionally a real BCI test with a PSK-based transceiver was performed. The setup is depicted in Fig. 12. The results are compared to the DPI simulation of the ASK transceiver model in Fig. 13 in order to validate the theoretical results from previous analysis.

Commonly used LIN transceivers are robust to such disturbances [21]. The curves in Fig. 13 represent the maximum immunity limit related to the injected forward power, depending on the frequency.

As expected from the previous input filter analysis in Section III, there is a significant immunity drop at the filter passband of the ASK transceiver models. Reduction of immunity out of band can be caused by noise when injected power cannot be compensated by the filter and leads to an increased voltage level in the demodulated signal. A close match of immunity drop to the BCI measurement can be observed in the pass band at 6.5 MHz. The disturbance is caused by a reduction of the SNR. Additional out of band immunity drops of the measurement can be observed. Similar results for a DPI test of a PSK model were validated

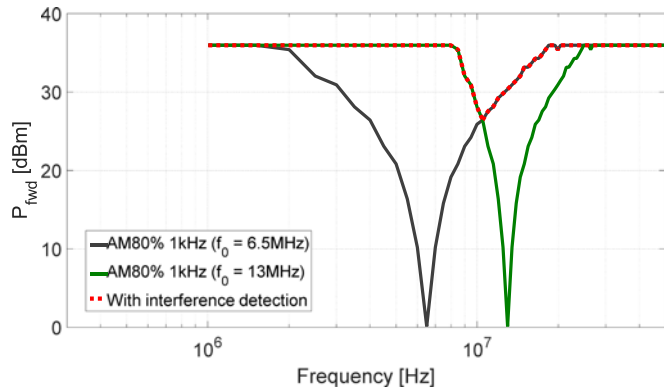


Fig. 14. Immunity limit with interference detection.

with measurements and discussed in [12]. Real implementations PLC transceiver inhibit problems not visible with ideal simulation models. An improved immunity curve can be achieved by using a better filter, such as the aforementioned Butterworth filter. Nevertheless, a PLC-system with these characteristics would not pass an immunity test. Therefore, further improvements are necessary, which will be discussed in the next section.

### C. Immunity Improvement by Interference Detection

Narrowband noise with high amplitude leads to an immunity drop in the pass band of the input filter as it has been shown in Section IV-B. Communication systems that use orthogonal frequency domain multiplexing usually have a much better performance in the presence of narrow band noise [22]. Other spread spectrum techniques could also improve the immunity. Unfortunately, such techniques are complex and expensive to implement, so some simple approaches are considered here instead. A simple interference detection with a set of operating frequencies can improve the EMC performance of a PLC that uses single carrier modulation.

Therefore, the transmitter models were modified and equipped with an additional receiving unit. This receiving unit scans the channel for pre-existing signals in the carrier frequency band before it sends the data. This method is similar to the [23] carrier sense multiple access/collision detection in PLC. The interference detection can be realized, e.g., by performing a cyclic redundancy check of the transmitted data in the transmitter or by requesting an acknowledge signal. In cases where interference is detected, the transmitter switches to an alternative frequency band. A multimaster network can also be realized, but this was not considered here.

The improved transceiver model uses two frequencies, 6.5 and 13 MHz, to implement a simple frequency domain multiplexing with interference detection as described before. For both frequencies the previously described second-order filters were applied. A DPI test was performed according to the setup shown in Fig. 11 with an AM modulated CW disturbance source. Fig. 14 shows the results of two single carrier PLC transceivers and one optimized dual carrier PLC transceiver with interference detection.

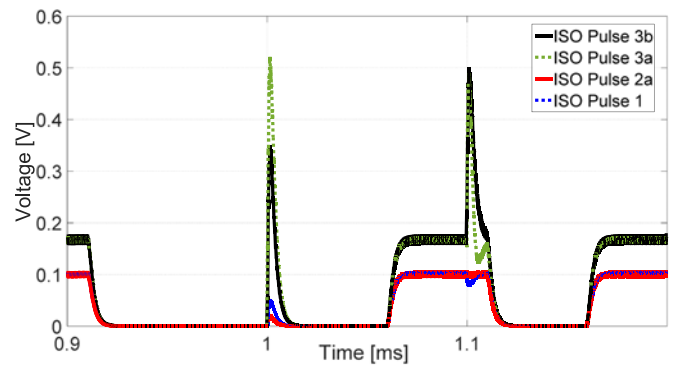


Fig. 15. Demodulated signal  $V_{\text{demod}}$  at the receiver from the ISO pulse test.

The optimized PLC system shows significant improvements in EMC robustness to the narrow band noise. Better input filters with higher orders for the respective bands can be used for further immunity improvements. The disadvantage of the approach shown here is that in cases where interference is detected, a data frame get lost and latency in data transmission might become critical.

### D. Transient Pulse Test and Analysis

The test of the immunity to pulses is also covered by automotive tests like the DPI [16] test. The virtual pulse DPI test was carried out according to Fig. 11. Here, instead of using a CW source, a pulse source was attached to inject different pulse shapes (ISO Pulse 1/2a/3a/3b) which are specified in [15]. The PLC model without interference and the second-order filter was tested. Even this simple investigated PLC transceiver model passed the test without any data errors. The injected ISO pulses have rise times up to 5 ns and magnitudes up to 220 V. A further time-domain analysis was performed for investigating the transmission of the pulses through the input filter and the demodulator in the model (see Fig. 10).

The results of the demodulated PLC signal  $V_{\text{demod}}$  with superimposed noise pulses are shown in Fig. 15. Due to the BP characteristic of the input filter, the injected pulse energy is small. Nevertheless, the pulses can be seen clearly in the signal shape. The high magnitudes of the pulse source are attenuated and do not exceed 0.6 V after passing the input filter and the demodulator.

Furthermore, the figure shows that the signal voltages of Pulses 1 and Pulse 2 are smaller than Pulse 3. According to the test standard [15], the source for Pulse 1 and 2 has an internal impedance of 10 and 2  $\Omega$ . The source for Pulse 3 has a source impedance of 50  $\Omega$ . Due to the increased load of the Pulse 1/2 source in the whole setup the magnitude decreases.

A detailed analysis can be performed by calculating the bit energy with following formula:

$$E_b = \int_{t_{\text{Bit start}}}^{t_{\text{Bit end}}} \frac{V(t)^2}{1 \Omega} dt. \quad (15)$$

The energy is normalized to 1  $\Omega$  to obtain the correct physical units. The results of this calculation, based on the signal voltages from Fig. 15, are listed in Table 1. The bit energy decision

TABLE 1  
BIT ENERGY IN PRESENCE OF PULSE DISTURBANCES

	Without Pulse (Pulse 1/2 source load)	Pulse 1	Pulse 2a	Without Pulse (Pulse 3 source load)	Pulse 3a	Pulse 3b
Bit0-Energy [J/Bit]	0	$3.2 \cdot 10^{-12}$	$1.6 \cdot 10^{-13}$	0	$2.9 \cdot 10^{-10}$	$1.3 \cdot 10^{-10}$
Decision- threshold [J/Bit]		$2.35 \cdot 10^{-7}$			$0.65 \cdot 10^{-6}$	
Bit1-Energy [J/Bit]	$4.7 \cdot 10^{-7}$	$0.5 \cdot 10^{-6}$	$0.5 \cdot 10^{-6}$	$1.3 \cdot 10^{-6}$	$1.6 \cdot 10^{-6}$	$1.9 \cdot 10^{-6}$

thresholds are based on voltage levels without disturbances, and they are calculated for the different pulse source impedance loads mentioned before.

From these calculations, it can be seen that pulse disturbances add energy to the bit states. The Bit0 energy should not exceed the decision threshold, and the Bit1 energy should not fall below the threshold for correct bit state detection. The calculations show no wrong bit decision because the threshold was not violated, and the simulation results confirm that.

## V. CONCLUSION

The objective of this paper was to investigate the important operation limits of PLC in an automotive environment in terms of immunity. Therefore, theoretical approximations of noise PSD and proposals for communication frequency bands, SNR and BER, were discussed. A conductive noise PSD of approximately  $-50$  dBm/Hz at a carrier frequency of 6.5 MHz can be expected in the 12-V vehicle power supply system. Furthermore, the noise power transmission of typical automotive component immunity test setups between the injection port and the PLC receiver were analyzed by investigating the model-based test setup. Additionally, the attenuation of different PLC input filters, combined with immunity setups, were analyzed. A virtual DPI test was performed with simple PLC models, based on ASK modulation and different input filters and compared to BCI measurements of a real transceiver. Interference detection was implemented on the transceiver models to increase the immunity level to narrow band noise. The final investigations on transient pulse disturbances show a good robustness of PLC to ISO-Pulses.

## REFERENCES

- [1] Y. Maryanka, "Wiring reduction by battery power line communication," in *Proc. Passenger Car Elect. Architect. IEE Semin.*, 2000, pp. 8/1–8/4.
- [2] J. Wolf, "Power line communication (PLC) in space—Current status and outlook," in *Proc. ESA Workshop Aerospace EMC*, May 2012, pp. 21–23.
- [3] F. Grassi *et al.*, "Design and SPICE simulation of coupling circuits for powerline communications onboard spacecraft," in *Proc. ESA Workshop Aerospace EMC*, 2012, pp. 1–6.
- [4] F. Grassi *et al.*, "Coupling/decoupling circuits for powerline communications in differential DC power buses," in *Proc. 16th IEEE Int. Symp. Power Line Commun. Appl.*, 2012, pp. 392–397.
- [5] W. Gouret *et al.*, "Powerline communication on automotive network," in *Proc. IEEE 65th Veh. Technol. Conf.*, 2007, pp. 2545–2549.
- [6] T. Huck *et al.*, "Tutorial about the implementation of a vehicular high speed communication system," in *Proc. IEEE Int. Symp. Power Line Commun. Appl.*, 2005, pp. 162–166.

- [7] M. Lienard *et al.*, "Modeling and analysis of in-vehicle power line communication channels," *IEEE Trans. Veh. Technol.*, vol. 57, no. 2, pp. 670–679, Mar. 2008.
- [8] M. O. Carrion *et al.*, "Communication over vehicular DC lines: Propagation channel characteristics," in *Proc. IEEE Int. Symp. Power Line Commun. Its Appl.*, Orlando, FL, USA, 2006, pp. 2–5.
- [9] A. Schiffer, "Statistical channel and noise modeling of vehicular DC-lines for data communication," in *Proc. IEEE 51st Veh. Technol. Conf.*, 2000, vol. 1, pp. 158–162.
- [10] V. Degardin *et al.*, "Impulsive noise characterization of in-vehicle power line," *IEEE Trans. Electromagn. Compat.*, vol. 50, no. 4, pp. 861–868, Nov. 2008.
- [11] Y. Yabuuchi *et al.*, "Low rate and high reliable modulation schemes for in-vehicle power line communications," in *Proc. IEEE Int. Symp. Power Line Commun. Appl.*, 2011, pp. 249–254.
- [12] A. Zeichner *et al.*, "Immunity of modulation schemes in automotive low bitrate power line communication systems," in *Proc. IEEE Int. Symp. Electromagn. Compat.*, 2015, pp. 743–748.
- [13] Regulation No 10 of the Economic Commission for Europe of the United Nations (UN/ECE)—Uniform provisions concerning the approval of vehicles with regard to electromagnetic compatibility, Official Journal of the European Union, 2010.
- [14] Vehicles, Boats and Internal Combustion Engines—Radio Disturbance Characteristics—Limits and Methods of Measurements for the Protection of On-board Receivers, CISPR 25, 2008.
- [15] Electrical transient conduction along supply lines only, ISO 7637–2, 2011.
- [16] EMC Evaluation of LIN Transceivers, IEC 622xx, Ed. 1/TS Draft 1.
- [17] C. E. Shannon, "Communication in the presence of noise," *Proc. IRE*, vol. 37, no. 1, pp. 10–21, 1949.
- [18] D. R. Smith, *Digital Transmission Systems*, 3rd ed. Norwell, MA, USA: Kluwer, 2004.
- [19] R. E. Collin, *Foundations for Microwave Engineering*. New York, NY, USA: Wiley, 2007.
- [20] F. M. Tesche *et al.*, *EMC Analysis Methods and Computational Models*. New York, NY, USA: Wiley, 1997.
- [21] P. Schröter *et al.*, "EMC compliant LIN transceiver," in *Proc. ESSCIRC*, 2013, pp. 363–366.
- [22] M. Tokuda *et al.*, "Conducted interference immunity characteristics to high-speed power line communication system," in *Proc. IEEE Int. Symp. Power Line Commun. Appl.*, 2011, pp. 118–123.
- [23] J. Taube *et al.*, "Real-time capabilities with digital powerline communications interfaces in CSMA/CD-networks," in *Proc. 3rd Int. Workshop Real-Time Netw.*, 2004, p. 85.



**Alexander Zeichner** received the B.M. and M.S. degrees in electrical engineering at the Technical University of Dortmund (TU Dortmund), Dortmund, Germany, in 2011 and 2013.

He is a Research Assistant at the On-board Systems Lab, TU Dortmund University. His main research interests include power line communication in vehicle and physical layer modeling and simulation of automotive bus systems.



**Stephan Frei** (M'97–SM'13) received the Dipl.-Ing. degree in electrical engineering from the Berlin University of Technology, Berlin, Germany, in 1995. He received the Ph.D. degree from the Institute of Electrical Power Engineering, Berlin University of Technology, in 1999.

Between 1995 and 1999, he was a Research Assistant for EMC at the Institute of Electrical Power Engineering, Berlin University of Technology. Between 1999 and 2006, he was at the automobile manufacturer AUDI AG in the development department.

Here, he developed and introduced new methods for the computation of EMC, antennas, and signal integrity in vehicles. Beginning in 2001, he and his team were responsible for the EMC release process of a type series and international standardization. In 2006, he became a Professor for vehicular electronics at TU Dortmund University, where his research interests include EMC, SI, computational methods, and vehicle power supply systems. He is the author of more than 150 papers, and from 2008 to 2009, he served as a Distinguished Lecturer for the IEEE EMC Society. He is currently the Dean of the Faculty for Electrical Engineering and Information Technology in Dortmund.